

# An Analysis of Temporal Dropout in Earth Observation Time Series for Regression Tasks

Miro Miranda<sup>1,2</sup>[0009-0002-8195-9776], Francisco Mena<sup>1,2</sup>[0000-0002-5004-6571],  
and Andreas Dengel<sup>1,2</sup>[0000-0002-6100-8255]

<sup>1</sup> University of Kaiserslautern-Landau, Kaiserslautern, Germany

<sup>2</sup> German Research Center for Artificial Intelligence, Kaiserslautern, Germany  
{miro.miranda\_lorenz, francisco.mena, andreas.dengel}@dfki.de

**Abstract.** Missing instances in time series data impose a significant challenge to deep learning models, particularly in regression tasks. In the Earth Observation field, satellite failure or cloud occlusion frequently results in missing time-steps, introducing uncertainties in the predicted output and causing a decline in predictive performance. While many studies address missing time-steps through data augmentation to improve model robustness, the uncertainty arising at the input level is commonly overlooked. To address this gap, we introduce Monte Carlo Temporal Dropout (MC-TD), a method that explicitly accounts for input-level uncertainty by randomly dropping time-steps during inference using a predefined dropout ratio, thereby simulating the effect of missing data. To bypass the need for costly searches for the optimal dropout ratio, we extend this approach with Monte Carlo Concrete Temporal Dropout (MC-ConcTD), a method that learns the optimal dropout distribution directly. Both MC-TD and MC-ConcTD are applied during inference, leveraging Monte Carlo sampling for uncertainty quantification. Experiments on three EO time-series datasets demonstrate that MC-ConcTD improves predictive performance and uncertainty calibration compared to existing approaches. Additionally, we highlight the advantages of adaptive dropout tuning over manual selection, making uncertainty quantification more robust and accessible for EO applications.

**Keywords:** Dropout · Earth Observation · Time Series · Regression · Uncertainty Quantification

## 1 Introduction

Recently, Deep Learning (DL) models have been widely used in the Earth Observation (EO) field to find optimal data-driven solutions in different applications [3]. DL effectively processes complex and heterogeneous sensor data, allowing for accurate analysis of environmental patterns [27]. For instance, predicting continuous values such as crop yield [38], water content in plants [39], and surface forecast [40] involves processing complex data. In the EO field, processing time series sensor data is essential for understanding the changes and dynamics of our planet [29]. However, sensors may experience anomalies and occlusions, leading

to missing data over certain time-steps [43,15,11]. For instance, clouds obstruct the sunlight in optical images, as on average, 67% of Earth’s surface is covered by clouds [22], often resulting in uncertain predicted outputs. Addressing missing data in time series is a prevalent challenge in the DL field, with various modeling solutions and pre-processing techniques developed to mitigate its impact and ensure accurate predictions. While various techniques exist to mitigate missing data [15,26], few explicitly quantify the uncertainty it introduces, particularly the impact of input-level uncertainty. Addressing this gap is crucial for improving model reliability in EO regression applications.

In this work, we analyze two models that simulate missing data across time series during training and inference for a dual purpose. During training, it acts as an augmentation technique to increase model generalization to missing data in temporal EO data. During inference, by generating multiple Monte Carlo (MC) samples with different missing patterns, it acts as an Uncertainty Quantification (UQ) mechanism, thereby increasing the trustworthiness of a prediction. The first model is built on the dropout variational distribution applied during inference [13] and over time, referred to as Monte Carlo Temporal Dropout (MC-TD). However, the optimal dropout value is a difficult hyperparameter to tune, requiring a resource-intensive process that depends on each dataset and missing data type [26]. Instead of manually searching, we propose using Concrete Dropout (ConcD) [14] to learn the optimal dropout ratio using standard gradient descent. We refer to this method as Monte Carlo Concrete Temporal Dropout (MC-ConcTD), where ConcD is applied across time and during inference. The ConcD [14] approximates a Bernoulli distribution using a continuous relaxation, enabling the dropout probability to be optimized through gradient-based learning [24]. Unlike traditional dropout-based approaches, this model automatically learns an optimal dropout distribution, eliminating costly hyperparameter tuning.

We validate MC-TD and MC-ConcTD on regression tasks spanning three EO datasets with temporal sensor data. Experimental results demonstrate that MC-ConcTD improves both predictive accuracy and uncertainty calibration, while also eliminating the need for manual dropout tuning. The Concrete Temporal Dropout (ConcTD) not only enhances predictive performance but also improves the accessibility and practicality of UQ in EO regression applications. The code is publicly available at <https://github.com/mmiranda-1/Temporal-Dropout/>.

## 2 Related Work

*Missing data in time series.* Irregular sampled time series are common in signal processing [36]. Temporal observations can easily suffer from problems in their collection, causing irregular observations with missing data. Numerous research in DL has focused on learning to impute time series, such as BRITS [4], mTAN [44], and SAITS [10], while others focused on adapting models to ignore the missing data, such as D-GRU [5] and MissFormer [1]. In the EO field, missing spatial and temporal data are a common phenomenon due to real-world data collection

constraints [43]. This includes, sensor noise, sensor failure, and cloud occlusion, affecting observations and introducing uncertainty. This problem negatively affects the performance of predictive models, where more missing data translates to worse predictions [20,12]. However, some strategies in the EO field mitigate the negative effect of missing data, such as including features from different sensors or using dropout techniques [35,15]. Recently, the Temporal Dropout (TD) technique, which involves randomly dropping time steps, has been used to enhance the model performance [15,47,18]. Furthermore, some studies leverage missing data as an augmentation technique to enhance generalization. For instance, Weitland et al. [50] randomly mask the end of a time-series for generalization to an early crop classification. On the other hand, some studies have focused on reconstruction tasks that recover the missing time-steps. For instance, Chen et al. [6] use a polynomial fit based on the Savitzky–Golay filter, while others use DL models based on Multi-layer Perceptron (MLP) [8], or convolutions [42].

*Regression with time series data.* Regression tasks have been lesser explored than classification tasks with time-series data [32]. One reason might be that DL models are not as effective for regression as for classification tasks, as shown by Tan et al. [46]. The intrinsic challenge of predicting a continuous value instead of a categorical value is often overlooked. Nevertheless, in the EO field, there are numerous applications involving pixel-level regression with time series data. For instance, Nguyen et al. [33] use multi-spectral data and weather time series for pixel-wise crop yield prediction. They use a MLP model for processing the time series data as individual features. However, it has been shown recently that Recurrent Neural Network (RNN) models obtain better results. This is underlined by [37,30]. Furthermore, Maimaitijiang et al. [25] consider the use of drone-based optical time series data for the same task, obtaining images unaffected by cloud occlusion. Another pixel-wise task studied in the literature is cloud removal. This task has been explored with multi-spectral optical time series data [41], as well as including radar time series [11]. Similarly, in the Earth surface forecast, multi-spectral optical and weather time series have been used with spatio-temporal models to obtain accurate predictions [40], such as using ConvLSTM models [9].

*Uncertainty estimation.* Uncertainty estimation holds particular promise in safety-critical applications, including the EO field [16]. Reliable uncertainty estimates improve decision-making by identifying predictions with high confidence and those that should be treated with caution [21,19]. Uncertainty in predictive models is typically classified into two categories: epistemic and aleatoric [21,19]. While the former captures the uncertainty coming from the model itself, the latter represents the uncertainty coming from the data exclusively, such as sensor noise. In regression, the aleatoric uncertainty is often directly learned from the data using proper scoring rules such as the Gaussian Negative Log-Likelihood (NLL) loss [34]. In contrast, epistemic uncertainty is typically estimated by modeling a distribution over the weight space, often based on Bayes’ Theorem. This

includes approximate Bayesian inference [2], or dropout techniques [13,14,31]. In the EO field, numerous studies have assessed the effectiveness of UQ methods, particularly in applications such as crop yield prediction with time series data, as evidenced in [23]. However, most of these studies overlook the uncertainty arising at the input level, which can be crucial in improving model reliability and robustness. In our work, we explore the simulation of missing data in EO time series for regression tasks. To the best of our knowledge, there is no method in the EO literature that accounts for the uncertainty arising from the input time series using missing time steps.

### 3 Temporal Dropout for Uncertainty Estimation

#### 3.1 Notation & Preliminaries

Let  $\mathbf{x} \in \mathcal{X}$  and  $y \in \mathcal{Y}$  denote samples from the input and target spaces, respectively. In the case of multivariate time series data with  $T$  time-steps,  $\mathbf{x}$  is given as  $\mathbf{x} = (x_0, \dots, x_T)$ . We further denote data pairs as  $(\mathbf{x}, y)$ , and define the goal to predict the target  $y$  from  $\mathbf{x}$ . Thus, we aim to find a model  $f^\theta(\cdot) : \mathcal{X} \mapsto \mathcal{Y}$  such that  $f^\theta(\mathbf{x}) = \hat{y}$ , by optimizing over the model’s parameters  $\theta$ .

*Uncertainty estimation:* We define the problem of learning the uncertainty in the predicted output ( $\hat{y} = \{\mu, \sigma^2\}$ ) propagated through the uncertainty in the input and the model itself. To estimate the epistemic uncertainty (EU), we model the expected output and variance over multiple stochastic forward passes, by placing a distribution over the network. Given independent input samples  $x^{(l)}$  drawn from the input distribution, EU is approximated as follows:

$$\begin{aligned} \mathbb{E}[f^\theta(x)] &= \mu_{EU} \approx L^{-1} \sum_l f^\theta(x^{(l)}) \\ \text{Var}[f^\theta(x)] &= \sigma_{EU}^2 \approx (L-1)^{-1} \sum_l (f^\theta(x^{(l)}) - \mathbb{E}[f^\theta(x)])^2. \end{aligned}$$

To estimate the aleatoric uncertainty (AU), which arises from the data, we assume a Normal distribution parameterized by two output heads:  $\mu(x), \sigma^2(x) = f^\theta(x)$ . Both terms can be optimized by minimizing the NLL [34]:

$$\mathcal{L}_{NLL}(y, x) = \log \sigma^2(x) + \frac{(\mu(x) - y)^2}{\sigma^2(x)}. \quad (1)$$

This approach captures AU in  $\sigma^2(x)$ , allowing the model to capture data related uncertainty. In Valdenegro-Toro et al. [49] a relationship between input and output uncertainty is given, showing that input uncertainty is propagated through the model, finally resulting in model, or epistemic uncertainty (EU) by leveraging stochastic MC sampling. We follow this argumentation. Finally, the predictive uncertainty (PU) is the combined effect of all uncertainties.

### 3.2 Temporal Dropout

We leverage TD to estimate uncertainty. The dropout technique [45] is commonly used in hidden layers of DL models during training. Nevertheless, applying this technique at the input-level across time has shown good regularization performance in the EO field [28,15,47,26,18]. This prevents the model from focusing on individual time-steps and simultaneously handling missing time-steps, which randomly occur in EO data with sensor failure and cloud coverage. Thus, the multivariate time series data  $\mathbf{x}$  is masked out as

$$\hat{\mathbf{x}} = \mathbf{x} \odot (1 - \mathbf{p}), \quad (2)$$

where  $\mathbf{p} \in [0, 1]^T$  is the binary dropout mask, which is drawn from a Bernoulli distribution, i.e.  $p_i \sim \text{Bern}(\alpha), \forall i = 1, \dots, T$ , with  $\alpha$  as the dropout ratio. Thus, the input  $\mathbf{x}$  becomes a random variable  $\hat{\mathbf{x}}$ , providing additional network regularization. In contrast, we estimate the uncertainty arising from missing time steps, by enabling TD at the inference level. Gal et al. [13] demonstrated that casting dropout approximates Bayesian inference in any neural network architecture. Similarly, we extend this formulation along the temporal dimension, named **Monte Carlo Temporal Dropout (MC-TD)**. This corresponds to sampling  $L$  different dropout masks for prediction,  $p_i^{(l)} \sim \text{Bern}(\alpha), \forall l = 1, \dots, L$ , and applying them to the input data as  $\hat{\mathbf{x}}^{(l)} = \mathbf{x} \odot (1 - \mathbf{p}^{(l)})$ .

### 3.3 Concrete Temporal Dropout

When using the TD technique, an optimal dropout ratio value ( $\alpha$ ) has to be identified to get a well-calibrated model. This is a computationally expensive and time-consuming process, especially when working with over-parametrized models, commonly used in the EO field and time series modeling. In Gal et al. [14] a continuous relaxation of the dropout technique is proposed, allowing the dropout ratio to be a learnable parameter in combination with standard gradient descent. The soft dropout mask  $\tilde{\mathbf{p}}$  is defined as:

$$\tilde{\mathbf{p}} = CS(\alpha, \mathbf{u}, \tau) = \sigma \left( \left( \log \frac{\alpha}{(1 - \alpha)} + \log \frac{\mathbf{u}}{(1 - \mathbf{u})} \right) \frac{1}{\tau} \right), \quad (3)$$

with  $\sigma$  the sigmoid function,  $\tau \in \mathbb{R}^1$  a temperature value controlling the smoothness of the approximation,  $\alpha \in \mathbb{R}^1$  a learnable parameter in the model, and  $\mathbf{u}$  a uniform random variable,  $u_i \sim \text{Uni}(0, 1), \forall i = 1, \dots, T$ . The latter acts as the auxiliary variable in the sampling reparametrisation [24]. We use this sampling strategy in the dropout across time, named Concrete Temporal Dropout (ConcTD). Furthermore, to get the uncertainty, we use this technique at inference time, referred to as **Monte Carlo Concrete Temporal Dropout (MC-ConcTD)**. This corresponds to obtaining  $L$  samples of the Uniform distribution,  $u_i^{(l)} \sim \text{Uni}(0, 1), \forall l = 1, \dots, L$ , and forward over the model with data as  $\hat{\mathbf{x}}^{(l)} = \mathbf{x} \odot (1 - CS(\alpha, \mathbf{u}^{(l)}, \tau))$ . This technique is illustrated in Figure 1. Additionally, in Figure 2 we schematically illustrate TD and ConcTD.

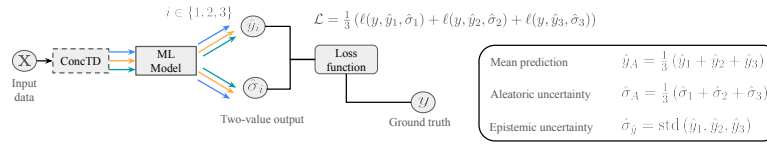


Fig. 1: Illustration of a DL model prediction with the ConcTD technique and three MC samples indexed by  $i \in \{1, 2, 3\}$ .

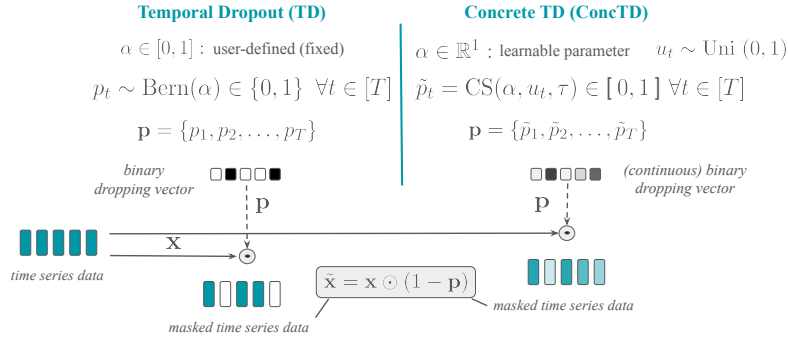


Fig. 2: Illustration of TD and ConcTD techniques over time series data.

## 4 Experiments

### 4.1 Datasets

We use three publicly available EO datasets with temporal sensor data. The characteristics of these datasets are presented in Table 1.

*Swiss Crop Yield (SwissYield)* We use a dataset for crop yield estimation [38], focused on cereals. This is a regression task in which the crop yield is estimated in tons per hectare (t/ha) from sensor data. The data was collected in Switzerland between 2017 and 2021. The temporal features are multi-spectral optical sensor (from Sentinel-2, with 10 bands) and weather data (with 5 bands). The time series are from seeding to harvesting, with an approximate 5 days of sampling rate. All features were spatially interpolated to a pixel resolution of 10 m.

*Live Fuel Moisture Content (LFMC)* We use a dataset for moisture content estimation [39]. This involves a regression task in which the vegetation water (moisture) per dry biomass (in percentage) in a given location is predicted. The data was collected between 2015 and 2019 in the western US. The temporal features are multi-spectral optical sensor (from Landsat-8, with 8 bands) and radar sensor (from Sentinel-1, with 3 bands). These features were re-sampled monthly during a four-month window before the moisture measurement, i.e. a signal of 4 time-steps is used. Additional static sensors are the topographic

Dataset	Samples	Series length	Features	Avg. target	Std. target
SwissYield	54,098	16-55	15	7.356	2.001
LFMC	2,578	4 (fixed)	61	103.987	39.562
PM2.5	167,309	120 (fixed)	9	73.673	68.546

Table 1: Datasets description and statistics.

information, soil properties, canopy height, and land-cover class. All features were interpolated to a pixel resolution of 250 m.

*Particles Matter 2.5 (PM2.5)* We use a dataset for PM2.5 estimation [7]. This involves a regression task in which the concentration of PM2.5 (particles measure 2.5 microns or fewer in diameter) in the air (in  $\mu g/m^3$ ) in a particular city is predicted. The data was collected between 2010 and 2015 in five Chinese cities. The temporal features are atmospheric conditions (with 3 bands), atmospheric dynamics (with 4 bands), and precipitation (with 2 bands). These are captured at hourly resolution, where we consider a three-day window for prediction.

## 4.2 Setup

We use an early fusion strategy that concatenates all features along the time steps. For the architecture, we adopt a RNN model with 2 layers based on long-short term memory units to extract the temporal information. Then, one additional layer is used to map the last hidden state of the RNN into a hidden dimension. Finally, two prediction heads are employed, reflecting the mean and variance, respectively. All layers consist of 128 units, including 20% of dropout. In addition, we use batch normalization layers after the RNN model. We train the models for 100 epochs with an early stopping criteria based on a patience of five. The optimization is carried out with the ADAM optimizer and a batch size of 128 over the Mean Squared Error (MSE) function. For MC sampling, 20 samples are used as in [13]. We first evaluate MC-TD and MC-ConcTD against each other and then against standard UQ methods for time series regression tasks, including MC-Dropout [13] and a Variational Inference (VI) [2]. For comparison, all models employ the same architecture. If not differently specified, a TD ratio of 0.3 is used for the MC-TD model, thereby aiming for a balance between regularization and model capacity.

## 4.3 Results

We compare the performance of MC-ConcTD and MC-TD models across all datasets in Table 2. Both approaches demonstrate strong performance across all three datasets. However, MC-ConcTD consistently outperforms MC-TD on all regression metrics for every dataset. For instance, a maximum improvement of 6 percentage points (p.p) is shown in  $R^2$  on the PM2.5 dataset.

In Figure 3 (a), we evaluate the performance of various dropout ratios in the MC-TD model. The results indicate that a lower dropout ratio consistently improves performance across all datasets, with a clear decline in model performance as the ratio increases. Additionally, we observe an increase in PU with increasing TD ratio and decreasing performance. In Figure 3 (b) the calibration error (ECE) for every TD ratio is illustrated, together with the constant ECE for the MC-ConcTD model. Marker sizes indicate normalized PU. Similarly, we observe an increase in calibration error with increased uncertainty, except for the SwissYield dataset, and decreased performance. Ultimately, in Figure 3 (c), the learned dropout ratios of the MC-ConcTD model across all folds and datasets are illustrated. Notably, the dropout ratios remain below 0.25 with significant instability across folds and datasets. For instance, approaching zero for the PM2.5 dataset. The results underline the difficulty of manually tuning the dropout ratio.

In Figure 4, we illustrate the model calibration. We define calibration as the models’ capabilities to accurately reflect the true probabilities of observed outcomes. For instance, for an 80% confidence level, an event should occur approximately 80% of the time. Ideally, a perfectly calibrated model aligns with the diagonal line. In the SwissYield and LPMC datasets, the models are overconfident, though the MC-ConcTD model demonstrates relatively better calibration overall. Conversely, for the PM2.5 dataset, the models exhibit better calibration, especially for the MC-ConcTD model. In Figure 5, prediction-versus-target plots

Dataset	Model	R2( $\uparrow$ )	RMSE( $\downarrow$ )	MAE( $\downarrow$ )	ECE( $\downarrow$ )	PU ( $\downarrow$ )
SwissYield	MC-TD	0.76	0.99	0.72	<b>2.14</b>	<b>1.00</b>
	MC-ConcTD	<b>0.79</b>	<b>0.93</b>	<b>0.66</b>	2.23	1.23
LFMC	MC-TD	0.69	21.92	15.67	3.77	<b>1.01</b>
	MC-ConcTD	<b>0.72</b>	<b>20.80</b>	<b>14.76</b>	<b>3.41</b>	8.01
PM2.5	MC-TD	0.71	36.36	24.56	2.92	16.00
	MC-ConcTD	<b>0.77</b>	<b>31.77</b>	<b>21.61</b>	<b>2.15</b>	<b>5.80</b>

Table 2: Results of the two variants of dropout across time. The best results are highlighted in bold. The MC-TD model uses a dropout ratio of 0.3.

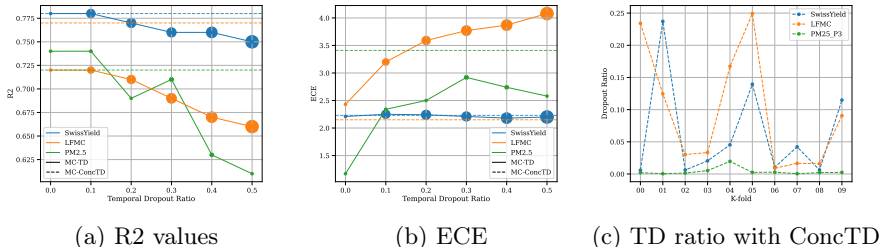


Fig. 3: Model performance in  $R^2$  and ECE under different TD settings, where marker size indicates the normalized PU.

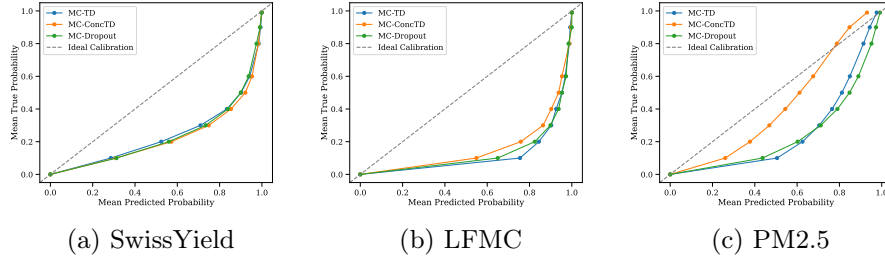


Fig. 4: Model calibration across confidence levels for all datasets.

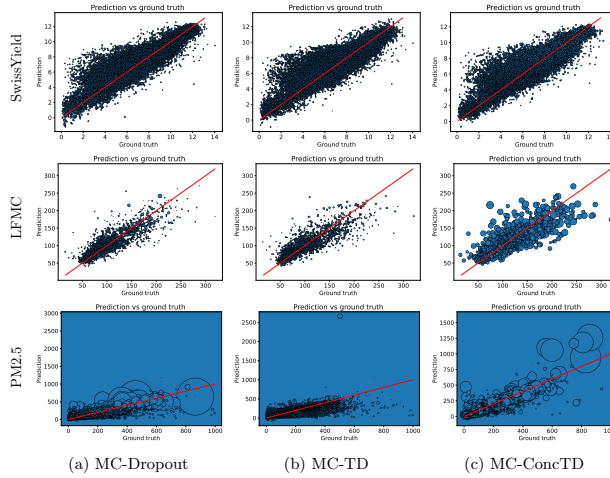


Fig. 5: Prediction over target plots for three regression datasets. The marker size indicates the uncertainty in each prediction.

are shown for MC-Dropout, the MC-TD, and MC-ConcTD models on the three datasets. To analyze uncertainty estimates, the predictions are scaled based on the PU. Overall, the plots show a good alignment between predicted and target values. However, the distinct characteristics of the datasets become evident, with the PM2.5 dataset exhibiting very high uncertainties and the SwissYield dataset showing consistently low uncertainties. Furthermore, we observe that higher uncertainties are associated with lower alignment between predicted and target values, particularly for the MC-ConcTD model.

Finally, we compare the introduced models against two established UQ methods, namely MC-Dropout and VI. The results are summarized in Table 3. Notably, the VI performs poorly on regression metrics. The MC-ConcTD model

Dataset	Model	R2 ( $\uparrow$ )	RMSE ( $\downarrow$ )	MAE ( $\downarrow$ )	ECE ( $\downarrow$ )	PU ( $\downarrow$ )
SwissYield	MC-Dropout	0.78	0.94	0.67	2.21	1.02
	MC-TD	0.76	0.99	0.72	2.14	<b>1.00</b>
	MC-ConcTD	<b>0.79</b>	<b>0.93</b>	<b>0.66</b>	2.23	1.23
	VI	0.51	2.02	1.57	<b>0.73</b>	23.57
LFMC	MC-Dropout	<b>0.72</b>	<b>20.69</b>	<b>14.64</b>	<b>2.43</b>	1.11
	MC-TD	0.69	21.92	15.67	3.77	<b>1.01</b>
	MC-ConcTD	<b>0.72</b>	20.80	14.76	3.41	8.01
	VI	0.53	27.00	20.00	4.48	4.01
PM2.5	MC-Dropout	0.74	33.89	22.45	<b>1.17</b>	3.99
	MC-TD	0.71	36.36	24.56	2.92	16.00
	MC-ConcTD	<b>0.77</b>	<b>31.77</b>	<b>21.61</b>	2.15	5.80
	VI	0.30	57.00	39.00	3.57	<b>2.49</b>

Table 3: Performance comparison for various UQ models.

achieves the best R2 scores on the SwissYield and PM2.5 datasets, while being equal to the MC-Dropout on the LFMC dataset. Considering all evaluation metrics, we find that the MC-ConcTD has the best overall results.

## 5 Discussion

We empirically prove that TD at the inference level improves model performance over common UQ methods on various EO regression tasks (Table 2 and Table 3), thereby confirming related studies [18]. However, calibrating the dropout ratio in any DL model is challenging as it requires exploring a continuous hyperparameter space. The same applies to the MC-TD method. Consequently, MC-TD can only find the optimal dropout ratio at high computational search costs. Interestingly, higher dropout ratios or missing time-steps consistently result in reduced performance with increased uncertainty and calibration error, with an optimum value of around 0.1. The optimal value must balance predictive performance, uncertainty, and calibration error. This underlines the need for effective management of missing instances. Particularly, when time windows are small, determining the optimal ratio remains challenging. Nevertheless, MC-ConcTD demonstrates adaptability by learning different values based on the validation scenario (fold). This adaptability arises from the model’s ability to dynamically adjust the dropout value using the ConcD [14], leading to improved performance and calibration. Nevertheless, we observe high variability across datasets. Moreover, we notice that there may be multiple optimal dropout ratios, as illustrated in Fig. 3 (c). For instance, for the SwissYield dataset, the learned ratio of the second fold is approximately 0.25, whereas in the sixth fold, it is approximately 0.01. We attribute this variability to the distinct characteristics of each dataset, including varying time series length, number of features, and dataset size (Table 1). For instance, the LFMC dataset is characterized by only four time steps, which could potentially explain the poor performance of TD-based models on

this dataset. In contrast, the PM2.5 dataset has 120 time steps, but has only short temporal dependencies compared to the SwissYield dataset. Therefore, dropping the previous time-steps can significantly reduce performance. As a result, TD is less effective in this context, potentially explaining the low TD ratios in Fig. 3 (c). Overall, ConcTD enhances the robustness of UQ across different EO datasets, by continuously adapting to unique data characteristics while reducing the computational burden of optimal ratio search, making UQ more accessible for EO applications with time series data.

**Limitations** The proposed methods and experimental setup have limitations that must be considered. We validate the models using EO data without real missing values in the time series, which could potentially differ from scenarios involving actual missing data. This limitation may affect how the models perform in real-world situations where missing values are present. Additionally, we use only an RNN encoder to learn the temporal patterns and only few UQ methods for comparison. However, the primary goal of this study is to demonstrate the effectiveness of TD and ConcTD in enhancing predictive performance and UQ, rather than identifying the optimal architecture for each dataset and use case. Nevertheless, additional models and architectures must be evaluated in the future, including Transformers, and other UQ methods. Moreover, while TD has shown significant improvements in related literature [18], we observe only small improvements in this study on individual datasets. This may be attributed to the task and the unique data characteristics, including short time series length (LFMC), short temporal dependencies (PM2.5), or noise in remote sensing data. More datasets must be considered to better understand the robustness of the proposed methods. Finally, while we demonstrate improvements in our models regarding the literature, we emphasize that poor calibration remains an ongoing challenge that requires careful evaluation, an issue commonly encountered in DL [17,48]. Specifically, EO data is often impacted by noisy and uncertain measurements and spatio-temporal distribution shifts, which can lead to poor calibration when the model is applied to unknown environments. Further exploring model calibration, including post-hoc calibration, will be required before deploying models into practice.

## 6 Conclusion

This work underscores the importance of input uncertainty in time-series data for EO regression applications. To address this, we introduced two novel uncertainty estimation methods, namely MC-TD and MC-ConcTD. Both methods account for input uncertainty in time series data by applying Temporal Dropout (TD) at the inference level using Monte Carlo sampling. While MC-TD requires manual and expensive tuning of the dropout ratio, MC-ConcTD learns this automatically as a free parameter. We empirically demonstrate their effectiveness in enhancing predictive performance in various EO datasets. While these models improve the accessibility of uncertainty estimation in EO applications, they also

present challenges that require further investigation. Future research will focus on validating these approaches across diverse EO applications and by considering model calibration.

**Acknowledgments.** We acknowledge the support of the University of Kaiserslautern-Landau (RPTU) and the German Research Center for Artificial Intelligence (DFKI).

**Disclosure of Interests.** The authors have no competing interests to declare that are relevant to the content of this article.

## References

1. Becker, S., Hug, R., Huebner, W., Arens, M., Morris, B.T.: Missformer:(in-) attention-based handling of missing observations for trajectory filtering and prediction. In: International Symposium on Visual Computing. pp. 521–533 (2021)
2. Blundell, C., Cornebise, J., Kavukcuoglu, K., et al.: Weight uncertainty in neural network. In: International Conference on Machine Learning. pp. 1613–1622 (2015)
3. Camps-Valls, G., Tuia, D., Zhu, X.X., Reichstein, M.: Deep learning for the Earth sciences: A comprehensive approach to remote sensing, climate science and geosciences. John Wiley & Sons (2021)
4. Cao, W., Wang, D., Li, J., Zhou, H., et al.: Brits: Bidirectional recurrent imputation for time series. *Advances in Neural Information Processing Systems* **31** (2018)
5. Che, Z., Purushotham, S., Cho, K., Sontag, D., Liu, Y.: Recurrent neural networks for multivariate time series with missing values. *Scientific reports* **8**(1), 6085 (2018)
6. Chen, J., Jönsson, P., Tamura, M., Gu, Z., Matsushita, B., Eklundh, L.: A simple method for reconstructing a high-quality NDVI time-series data set based on the Savitzky–Golay filter. *Remote Sensing of Environment* **91**(3-4), 332–344 (2004)
7. Chen, S.: PM2.5 Data of Five Chinese Cities. UCI Machine Learning Repo. (2017)
8. Das, M., Ghosh, S.K.: A deep-learning-based forecasting ensemble to predict missing data for remote sensing analysis. *IEEE Journal of Selected Topics in Applied Earth Observations and Remote Sensing* **10**(12), 5228–5236 (2017)
9. Diaconu, C.A., Saha, S., Günnemann, S., et al.: Understanding the role of weather data for earth surface forecasting using a ConvLSTM-based model. In: IEEE/CVF Conference on Computer Vision and Pattern Recognition. pp. 1362–1371 (2022)
10. Du, W., Côté, D., Liu, Y.: Saits: Self-attention-based imputation for time series. *Expert Systems with Applications* **219**, 119619 (2023)
11. Ebel, P., Garnot, V.S.F., Schmitt, M., et al.: UnCRtainTS: Uncertainty quantification for cloud removal in optical satellite time series. In: IEEE/CVF Conference on Computer Vision and Pattern Recognition. pp. 2086–2096 (2023)
12. Ferrari, F., Ferreira, M.P., Almeida, C.A., Feitosa, R.Q.: Fusing Sentinel-1 and Sentinel-2 images for deforestation detection in the Brazilian Amazon under diverse cloud conditions. *IEEE Geoscience and Remote Sensing Letters* **20**, 1–5 (2023)
13. Gal, Y., Ghahramani, Z.: Dropout as a Bayesian approximation: Representing model uncertainty in deep learning. In: International Conference on Machine Learning. pp. 1050–1059 (2016)
14. Gal, Y., Hron, J., Kendall, A.: Concrete dropout. *Advances in Neural Information Processing Systems* **30** (2017)

15. Garnot, V.S.F., Landrieu, L., Chehata, N.: Multi-modal temporal attention models for crop mapping from satellite time series. *ISPRS Journal of Photogrammetry and Remote Sensing* **187**, 294–305 (2022)
16. Gawlikowski, J., Tassi, C.R.N., Ali, M., Lee, J., Humt, M., Feng, J., Kruspe, A., Triebel, R., Jung, P., Roscher, R., et al.: A survey of uncertainty in deep neural networks. *Artificial Intelligence Review* **56**(Suppl 1), 1513–1589 (2023)
17. Guo, C., Pleiss, G., Sun, Y., Weinberger, K.Q.: On calibration of modern neural networks. In: *International Conference on Machine Learning*. pp. 1321–1330 (2017)
18. Helber, P., Bischke, B., Packbier, C., Habelitz, P., Seefeldt, F.: An operational approach to large-scale crop yield prediction with spatio-temporal machine learning models. In: *IGARSS 2024-2024 IEEE International Geoscience and Remote Sensing Symposium*. pp. 4299–4302. IEEE (2024)
19. Hüllermeier, E., Waegeman, W.: Aleatoric and epistemic uncertainty in machine learning: An introduction to concepts and methods. *Machine Learning* **110**, 457–506 (2021)
20. Inglada, J., Vincent, A., Arias, M., Marais-Sicre, C.: Improved early crop type identification by joint use of high temporal resolution SAR and optical image time series. *Remote Sensing* **8**(5), 362 (2016)
21. Kendall, A., Gal, Y.: What uncertainties do we need in Bayesian deep learning for computer vision? *Advances in Neural Information Processing Systems* **30** (2017)
22. King, M.D., Platnick, S., Menzel, W.P., Ackerman, S.A., Hubanks, P.A.: Spatial and temporal distribution of clouds observed by MODIS onboard the Terra and Aqua satellites. *IEEE Transactions on Geoscience and Remote Sensing* **51**(7), 3826–3852 (2013)
23. Ma, Y., Zhang, Z., Kang, Y., Özdoğan, M.: Corn yield prediction and uncertainty analysis based on remotely sensed variables using a bayesian neural network approach. *Remote Sensing of Environment* **259**, 112408 (2021)
24. Maddison, C.J., Mnih, A., Teh, Y.W.: The Concrete distribution: A continuous relaxation of discrete random variables. In: *International Conference on Learning Representations* (2017)
25. Maimaitijiang, M., Sagan, V., Sidike, P., Hartling, S., Esposito, F., Fritschi, F.B.: Soybean yield prediction from UAV using multimodal data fusion and deep learning. *Remote Sensing of Environment* **237**, 111599 (2020)
26. Mena, F., Arenas, D., Dengel, A.: Increasing the robustness of model predictions to missing sensors in earth observation. *arXiv preprint arXiv:2407.15512* (2024)
27. Mena, F., Arenas, D., Nuske, M., Dengel, A.: Common practices and taxonomy in deep multi-view fusion for remote sensing applications. *IEEE Journal of Selected Topics in Applied Earth Observations and Remote Sensing* pp. 4797 – 4818 (2024)
28. Metzger, N., Turkoglu, M.O., D’Aronco, S., Wegner, J.D., Schindler, K.: Crop classification under varying cloud cover with neural ordinary differential equations. *IEEE Transactions on Geoscience and Remote Sensing* **60**, 1–12 (2021)
29. Miller, L., Pelletier, C., Webb, G.I.: Deep learning for satellite image time-series analysis: A review. *IEEE Geoscience and Remote Sensing Magazine* (2024)
30. Miranda, M., Pathak, D., Nuske, M., Dengel, A.: Multi-modal fusion methods with local neighborhood information for crop yield prediction at field and subfield levels. In: *IGARSS 2024-2024 IEEE International Geoscience and Remote Sensing Symposium*. pp. 4307–4311. IEEE (2024)
31. Mobiny, A., Yuan, P., Moulik, S.K., Garg, N., Wu, C.C., Van Nguyen, H.: Drop-connect is effective in modeling uncertainty of bayesian deep networks. *Scientific reports* **11**(1), 5458 (2021)

32. Mohammadi Foumani, N., Miller, L., Tan, C.W., Webb, G.I., Forestier, G., Salehi, M.: Deep learning for time series classification and extrinsic regression: A current survey. *ACM Computing Surveys* **56**(9), 1–45 (2024)
33. Nguyen, L.H., Zhu, J., Lin, Z., Du, H., Yang, Z., Guo, W., Jin, F.: Spatial-temporal multi-task learning for within-field cotton yield prediction. In: *Advances in Knowledge Discovery and Data Mining*. pp. 343–354 (2019)
34. Nix, D.A., Weigend, A.S.: Estimating the mean and variance of the target probability distribution. In: *IEEE International Conference on Neural Networks*. vol. 1, pp. 55–60 (1994)
35. Ofori-Ampofo, S., Pelletier, C., Lang, S.: Crop type mapping from optical and radar time series using attention-based deep learning. *Remote Sensing* **13**(22), 4668 (2021)
36. Orfanidis, S.J.: *Introduction to signal processing*. Prentice-Hall, Inc. (1995)
37. Pathak, D., Miranda, M., Mena, F., Sanchez, C., et al.: Predicting crop yield with machine learning: An extensive analysis of input modalities and models on a field and sub-field level. In: *IEEE International Geoscience and Remote Sensing Symposium*. pp. 2767–2770 (2023)
38. Perich, G., Turkoglu, M.O., Graf, L.V., Wegner, J.D., Aasen, H., Walter, A., Liebisch, F.: Pixel-based yield mapping and prediction from Sentinel-2 using spectral indices and neural networks. *Field Crops Research* **292**, 108824 (2023)
39. Rao, K., Williams, A.P., Flefil, J.F., Konings, A.G.: SAR-enhanced mapping of live fuel moisture content. *Remote Sensing of Environment* **245**, 111797 (2020)
40. Requena-Mesa, C., Benson, V., Reichstein, M., Runge, J., Denzler, J.: Earthnet2021: A large-scale dataset and challenge for Earth surface forecasting as a guided video prediction task. In: *IEEE/CVF Conference on Computer Vision and Pattern Recognition*. pp. 1132–1142 (2021)
41. Sarukkai, V., Jain, A., UzKent, B., Ermon, S.: Cloud removal from satellite images using spatiotemporal generator networks. In: *IEEE/CVF Winter Conference on Applications of Computer Vision*. pp. 1796–1805 (2020)
42. Scarpa, G., Gargiulo, M., Mazza, A., Gaetano, R.: A CNN-based fusion method for feature extraction from Sentinel data. *Remote Sensing* **10**(2), 236 (2018)
43. Shen, H., Li, X., Cheng, Q., Zeng, C., Yang, G., Li, H., Zhang, L.: Missing information reconstruction of remote sensing data: A technical review. *IEEE Geoscience and Remote Sensing Magazine* **3**(3), 61–85 (2015)
44. Shukla, S.N., Marlin, B.: Multi-time attention networks for irregularly sampled time series. In: *International Conference on Learning Representations* (2021)
45. Srivastava, N., Hinton, G., Krizhevsky, A., Sutskever, I., Salakhutdinov, R.: Dropout: A simple way to prevent neural networks from overfitting. *Journal of Machine Learning Research* **15**(1), 1929–1958 (2014)
46. Tan, C.W., Bergmeir, C., Petitjean, F., Webb, G.I.: Time series extrinsic regression: Predicting numeric values from time series data. *Data Mining and Knowledge Discovery* **35**(3), 1032–1060 (2021)
47. Tseng, G., Cartuyvels, R., Zvonkov, I., Purohit, M., Rolnick, D., Kerner, H.R.: Lightweight, pre-trained transformers for remote sensing timeseries. In: *NeurIPS 2023 Workshop on Tackling Climate Change with Machine Learning* (2023)
48. Valdenegro-Toro, M.: I find your lack of uncertainty in computer vision disturbing. In: *Proceedings of the IEEE/CVF Conference on Computer Vision and Pattern Recognition*. pp. 1263–1272 (2021)
49. Valdenegro-Toro, M., de Jong, I.P., Zulloch, M.: Unified uncertainties: Combining input, data and model uncertainty into a single formulation. *arXiv e-prints* pp. arXiv–2406 (2024)

50. Weilandt, F., Behling, R., Goncalves, R., Madadi, A., Richter, L., Sanona, T., Spengler, D., Welsch, J.: Early crop classification via multi-modal satellite data fusion and temporal attention. *Remote Sensing* **15**(3), 799 (2023)